

Proceeding Paper

Particle Swarm Optimization Algorithm for Gold Nanohole Array Design [†]

Francesco Floris ^{*}, Margherita Angelini and Franco Marabelli

Department of Physics, University of Pavia, Via Bassi 6, 27100 Pavia, Italy;
margherita.angelini01@universitadipavia.it (M.A.); franco.marabelli@unipv.it (F.M.)

^{*} Correspondence: francesco.floris@unipv.it

[†] Presented at the 4th International Online Conference on Nanomaterials, 5–19 May 2023;
Available online: <https://iocn2023.sciforum.net>.

Abstract: Gold nanohole arrays represent a class of bidimensional plasmonic metasurfaces suitable for realizing optical sensors. We propose a modeling approach based on a customized particle swarm optimization algorithm implemented in the commercial Ansys Lumerical FDTD software. Providing the relevant optical and morphological parameters, we obtain a set of optimized geometrical parameters tailored to the required features. Specifically, we deal with square and hexagonal arrays of air cylinders embedded in a gold layer deposited on a glass substrate engineered for surface plasmon resonance technique-based biosensors. Two structures have been defined and are planned to be fabricated to validate our design routine.

Keywords: FDTD simulation; particle swarm optimization algorithm; gold nanohole arrays

1. Introduction

Gold Nanohole Arrays (GNAs) represent a class of hybrid metal/dielectric metasurfaces made of periodically arranged air holes drilled in a thick gold film. GNAs ability to support both localized and propagating surface plasmons [1] gives them good performances for surface plasmon resonance (SPR) oriented applications [2–5].

To optically tune these arrays, several algorithms can be used. Among them, the particle swarm optimization (PSO) algorithm [6,7] represents a powerful and versatile tool for the design of complex photonic structures [8,9] thanks to its intuitive mathematical structure, giving total control of the physical phenomena. This represents a major advantage with respect to other classes of evolutionary algorithms, such as genetic algorithms [9].

In this work, we resorted to a customized PSO algorithm implemented in Ansys Lumerical FDTD [10] where the GNAs were treated as 2D gratings following the Bragg-condition. The PSO was used to tune the spectral position of the minimum reflectance value at 770 nm, set as tuning wavelength, accordingly to the requirements of the project H2020 h-ALO [11]. The algorithm was then tailored to maximize the coupling of the source power into the main plasmonic resonance for two arrays, square and hexagonal. The PSO algorithm convergence and evolution were studied, and a mathematical model was developed to read its outcomes. The mismatch in the Bragg condition to the approximate estimations intrinsically carried by the FDTD method, was corrected through an iterative process inspired by [12,13].

2. Materials and Methods

The PSO evolutionary flow is schematically described in Figure 1. As a starting point, a general GNA structure is defined in the FDTD framework. Two parameters are defined to describe the GNA geometrical features, specifically the array pitch (P) and cylinder

Citation: Floris, F.; Angelini, M.; Marabelli, F. Particle Swarm Optimization Algorithm for Gold Nanohole Array Design. *Mater. Proc.* **2023**, *14*, x.
<https://doi.org/10.3390/xxxxx>
Published: 5 May 2023



Copyright: © 2023 by the authors. Submitted for possible open access publication under the terms and conditions of the Creative Commons Attribution (CC BY) license (<https://creativecommons.org/licenses/by/4.0/>).

radius (R). Two additional parameters, the velocity for both R and P, are set to manage the swarm evolution. These four parameters are randomly generated by the algorithm where R and P are used to build the different 3D FDTD structures, while the velocities are used to update the R and P values ensuring these are falling correctly within the chosen parameter space. For each (R, P) couple, defined as agent, the corresponding simulation is run and the Reflectance (Refl.) and Transmittance (Tran.) spectra are calculated. Finally, the algorithm evaluates the Fitness Function defined as:

$$FF = 1 - \text{Refl.} - \text{Tran.} \quad (1)$$

that can be related to the coupling efficiency of the incident source in pumping the plasmonic modes. Specifically, the algorithm maximizes the FF value with the constraint of the tuning wavelength belonging to the interval (770 ± 25) nm. The allowable FF values are compared until the highest is found through all the iterations for the whole swarm, i.e., the entire collection of agents. In the end, the couple (Best R, Best P) identify the structure with the highest and well-tuned FF. In this case “best” means the best FDTD structure that can be built by the PSO algorithm.

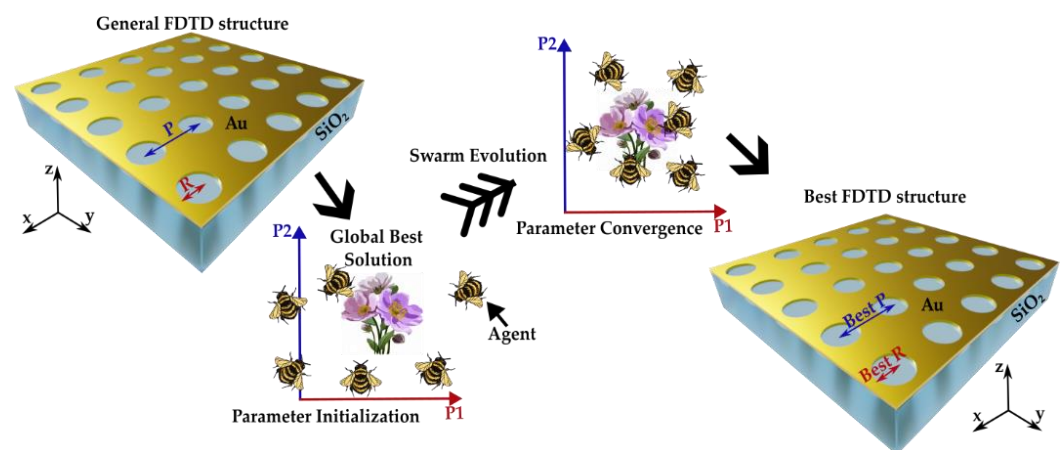


Figure 1. Process flow diagram of the Particle Swarm Optimization algorithm (left to right). A general FDTD structure can be mathematically defined by a point in the 2D parameter space, called agent, whose coordinates are given by Pitch (P) and Radius (R) values. Then, in the evolution process, the algorithm seeks in the whole space the best set of parameters (Best P, Best R) to obtain an FDTD structure that maximizes the numerical value of the selected fitness function within the imposed spectral position for the tuning wavelength.

For each specific array disposition, air cylinders are constructed on a semi-infinite SiO₂ substrate, embedded in a gold layer. Both cylinders and substrate are modeled as perfectly dielectric materials with a refractive index of 1 and 1.5, respectively, while the gold layer optical properties are set by the built-in Johnson and Christy data in the material database. A plane wave source, linearly polarized along the metasurface plane, is used to illuminate the structure from the substrate side at normal incidence with a spectral interval from $(650 \div 900)$ nm.

Due to the symmetry properties, the boundary conditions of the FDTD box were set to be antisymmetric along the x direction, symmetric along the y direction, and a perfectly matched layer along the z direction.

After performing convergency tests, an auto non-uniform mesh type with a five-mesh accuracy was set. According to Lumerical guidelines, due to the presence of metal/dielectric interfaces, conformal variant 2 mesh refinement was selected. To improve the simulation accuracy, a mesh override with a 4 nm resolution along the x-, y-, and z-directions was placed in correspondence of the GNA structure. Two frequency domain and power monitors, placed behind the source and above the gold layer, were used to record the Refl. and Tran. Spectra in the same spectral range.

The simulations were run on a liquid-cooled Intel® Core 12th generation i7-12700K (12 core) and 64 GB of DDR5-RAM and a liquid-cooled Intel® Core 12th generation i9-12900K (16 core) with 128 GB of DDR5-RAM. An average simulation time of about 6 h for the square array were required on the i7 while about 10 h were required for the hexagonal arrays on the i9. Table 1 reports the PSO parameters, together with the FF values and spectral positions, called λ_{best} .

Table 1. PSO parameters and results for the square and hexagonal GNAs.

Array	Agents	Iterations	R Range (nm)	P Range (nm)	Best R (nm)	Best P (nm)	λ_{best} (nm)
Square	15	20	75–125	400–500	97	454	763
Hexagonal	15	40	80–120	500–540	97	525	776

3. Results and Discussion

In Figure 2 the agents' velocities are plotted as a function of the iteration number for the square and hexagonal arrays, panels (a) and (b), respectively and the evolution analysis suggests that the PSO algorithm has reached the convergence. This can be understood by considering the asymptotic behavior towards the point (0,0), meaning that the algorithm is no more evolving. Panels (b) and (d) show the same concept in relation to the FF distribution in the parameter space. At convergence, the agents start swarming around the attractor within its basin of attraction, indicating that the best FF value, compatibly with the constraint on the tuning wavelength has been reached. The corresponding (Best R, Best P) set can be used to build the best FDTD structure.

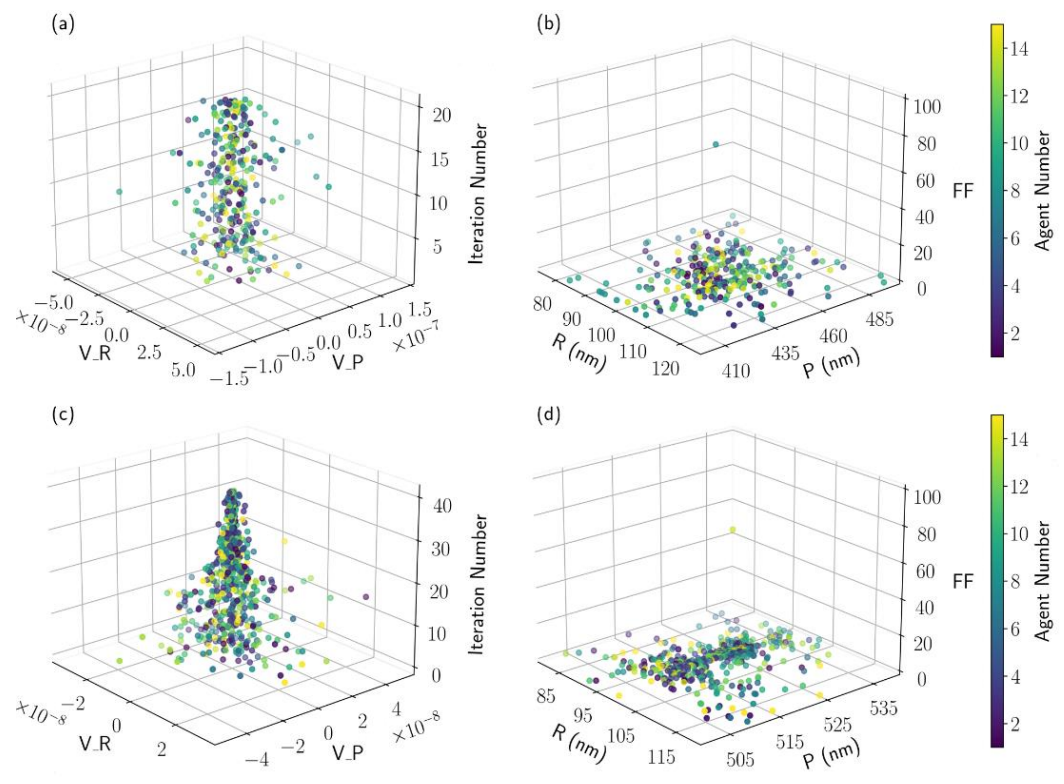


Figure 2. 3D scatter plot of the velocities associated with the PSO algorithm parameters (V_R , V_P) with respect to the iteration number for the square (panel (a)) and the hexagonal arrays (panel (c)). In panels (b,d) is reported the FF evolution in the R and P parameter space, for the square and hexagonal array, respectively. The agent number is labelled by the color.

At this stage, we need to go beyond the best that the PSO can provide to precisely tune the spectral position of the minimum reflectance value at 770 nm. As a starting point, we performed a sweep on Best P. Considering a similar sweep on Best R, we obtained several (R, P) couples used to build the corresponding GNA structures and calculate the respective reflectance spectra. In Figure 3 the scatter plot of the tuning wavelengths for the different p values considered in the sweep are reported as an example, for the hexagonal array.

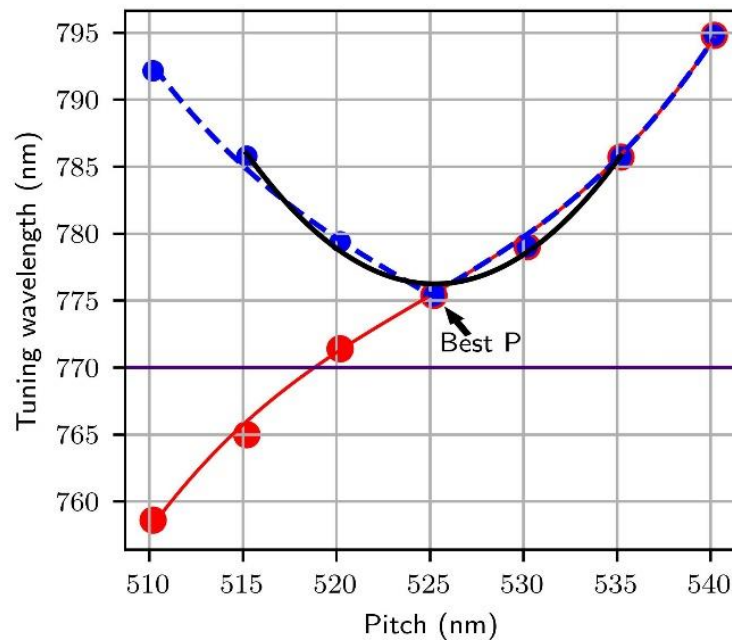


Figure 3. Tuning wavelengths for the sweep P points and the corresponding third order polynomial fit (in red). The mirrored points and their new behavior are reported in blue. The black curve indicates the parabolic approximation.

At this point we performed a polynomial fit finding the third order being able to describe properly the behavior. It can be seen that the Best P represents the inflection point of the polynomial curve. Thus, the retuning of the FF for the best FDTD structure means that the Best P must correspond to a tuning wavelength equal to 770 nm. This means a shift of the whole polynomial curve. Since, in addition, for GNAs, the main plasmonic resonance tuning depends also on R, we considered to build a retuning procedure based on the ratio between R and P. From the practical point of view, a smart way lies in mirroring the tuning wavelength values for the P points smaller than Best P with respect to its tuning wavelength. In this way, the inflection point becomes a corner and in its close neighborhood, the new curve can be approximated by a parabola. So, the corner point is now corresponding to the stationary point of the parabola, easier to be shifted, consequently retuning the wavelength for the best FDTD structure. For this reason, we took the p value for 770 nm, called P_{tuned} , and we calculated the corresponding R_{tuned} as:

$$R_{\text{tuned}} = R_{\text{best}} * P_{\text{tuned}}/P_{\text{best}} \quad (2)$$

At this point, we retuned the two arrays and the results are depicted in Figure 4, panels (a) and (d). Considering the first derivative, it was easy to identify the stationary point, shifting it in the right way applying Equation (2) and compensating for the R dependence of the plasmonic mode by slightly adjusting the R_{tuned} as shown in panels (b) and (e). The tuned R and P were used to compute the Refl., plotted in panels (c) and (f). It can be observed that the minimum is properly tuned at 770 nm for both the arrays.

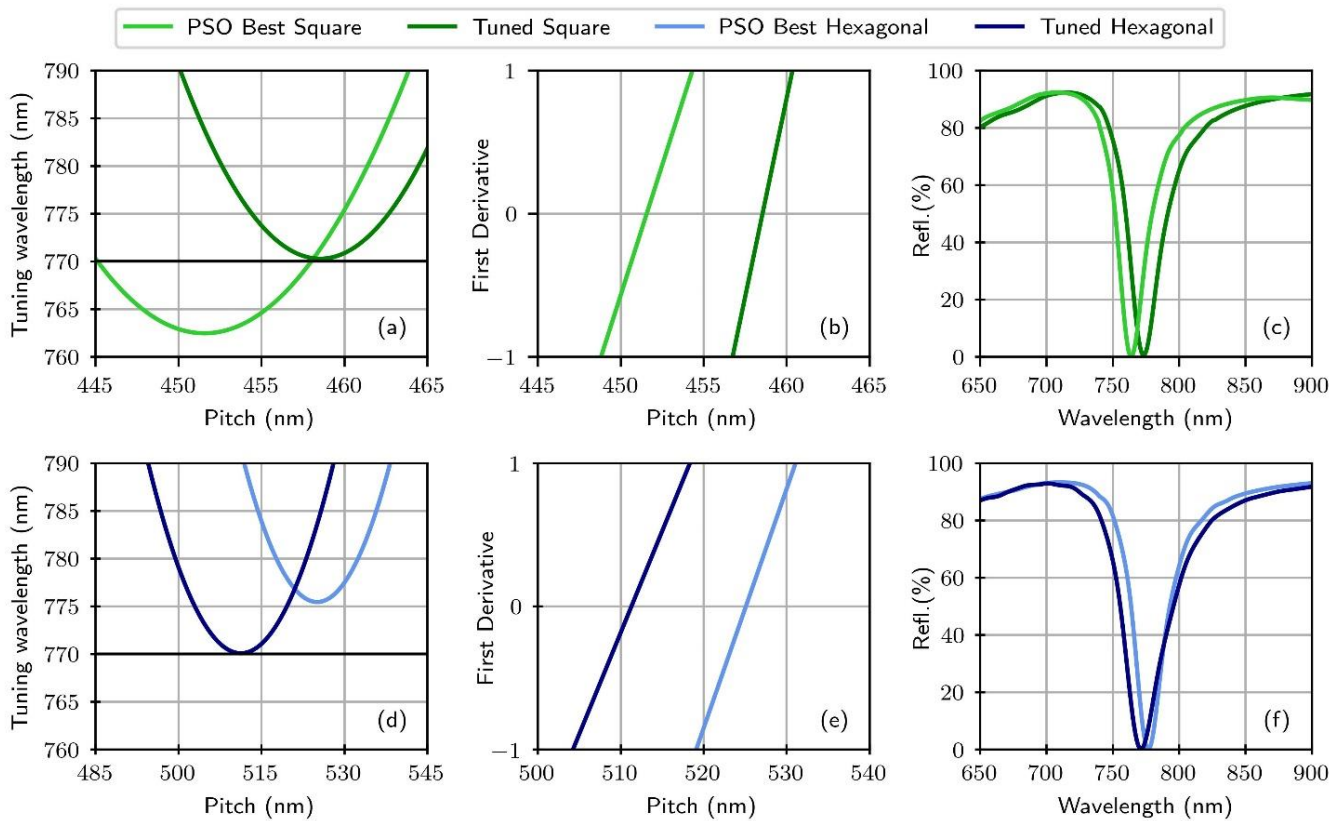


Figure 4. Results of the retuning procedure for the square (first row) and hexagonal (second row) arrays: evolution of the tuning wavelength (Refl. Minimum) as a function of the array Pitch panels (a,d)); first derivative of the parabolic curves (panels (e,f)); Reflectance curves of the optimized and tuned FDTD structures (panels (c,f)).

4. Conclusions

A design routine for the tuning of GNAs was developed based on a custom PSO algorithm implemented in the commercial FDTD software. A mathematical model has been defined to describe the evolution of the PSO and consequently retune its best solution. The design routine has been applied on both square and hexagonal arrays and two corresponding well-tuned structures have been obtained.

Author Contributions: Conceptualization, F.F. and F.M.; methodology, F.F.; software, F.F. and M.A.; validation, F.F., M.A. and F.M.; formal analysis, F.F. and M.A.; investigation, M.A. and F.F.; resources, F.F. and F.M.; data curation, M.A.; writing—original draft preparation, M.A. and F.F.; writing—review and editing, M.A., F.F. and F.M.; visualization, F.F., M.A. and F.M.; supervision, F.F. and F.M.; project administration, F.M.; funding acquisition, F.M. All authors have read and agreed to the published version of the manuscript.

Funding: This research was co-funded by the European Union’s Horizon 2020 project h-ALO (phonic system for Adaptable muLtipLe-analyte Monitoring of fOod quality), grant agreement No 101016706.

Institutional Review Board Statement: Not applicable.

Informed Consent Statement: Not applicable.

Data Availability Statement: Not applicable.

Conflicts of Interest: The authors declare no conflict of interest.

References

1. Martin-Moreno, L.; Garcia-Vidal, F.J.; Lezec, H.J.; Pellerin, K.M.; Thio, T.; Pendry, J.B.; Ebbesen, T.W. Theory of extraordinary optical transmission through subwavelength hole arrays. *Phys. Rev. Lett.* **2001**, *86*, 1114. <https://doi.org/10.1103/PhysRevLett.86.1114>.
2. Brolo, A.G.; Gordon, R.; Leathem, B.; Karen; Kavanagh, L. Surface Plasmon Sensor Based on the Enhanced Light Transmission through Arrays of Nanoholes in Gold Films. *Langmuir* **2004**, *20*, 4813–4815. <https://doi.org/10.1021/la0493621>.
3. Sun, L.L.; Leo, Y.S.; Zhou, X.; Ng, W.; Wong, T.I.; Deng, J. Localized surface plasmon resonance based point-of-care system for sepsis diagnosis. *Mater. Sci. Energy Technol.* **2020**, *3*, 274–281. <https://doi.org/10.1016/j.mset.2019.10.007>.
4. Escobedo, C. On-chip nanohole array based sensing: A review. *Lab A Chip* **2013**, *13*, 2445–2463. <https://doi.org/10.1039/C3LC50107H>.
5. Bottazzi, B.; Fornasari, L.; Frangolho, A.; Giudicatti, S.; Mantovani, A.; Marabelli, F.; Valsesia, A. Multiplexed label-free optical biosensor for medical diagnostics. *J. Biomed. Opt.* **2014**, *19*, 017006. <https://doi.org/10.1117/1.JBO.19.1.017006>.
6. Robinson, J.; Rahmat-Samii, Y. Particle swarm optimization in electromagnetics. *IEEE Trans. Antennas Propag.* **2004**, *52*, 397–407. <https://doi.org/10.1109/TAP.2004.823969>.
7. Rahmat-Samii, Y. Genetic algorithm (GA) and particle swarm optimization (PSO) in engineering electromagnetics. In Proceedings of the 17th International Conference on Applied Electromagnetics and Communications, Dubrovnik, Croatia, 1–3 October 2003; pp. 1–5. <https://doi.org/10.1109/ICECOM.2003.1290941>.
8. Zagaglia, L.; Floris, F.; O'Brien, P.A. Experimental Characterization of Particle Swarm Optimized Focusing Non-Uniform Grating Coupler for Multiple SOI Thicknesses. *JLT* **2021**, *39*, 5028–5034. <https://doi.org/10.1109/JLT.2021.3079575>.
9. Zagaglia, L.; Floris, F.; O'Brien, P. Optimized Design Procedure for Low-cost Grating-couplers in Photonics-packaging. In Proceedings of the 2019 Photonics & Electromagnetics Research Symposium—Spring (PIERS-Spring), Rome, Italy, 17–20 June 2019; pp. 234–241. <https://doi.org/10.1109/PIERS-Spring46901.2019.9017442>.
10. Lumerical Inc. Available online: <https://www.lumerical.com/products/fdtd/> (accessed on 20 February 2022).
11. Title. Available online: <https://cordis.europa.eu/project/id/101016706/it> (accessed on).
12. Zagaglia, L.; Demontis, V.; Rossella, F.; Floris, F. Particle swarm optimization of GaAs-AlGaAs nanowire photonic crystals as two-dimensional diffraction gratings for light trapping. *Nano Express* **2022**, *3*, 021001. <https://doi.org/10.1088/2632-959X/ac61ec>.
13. Passoni, M.; Floris, F.; Hwang, H.Y.; Zagaglia, L.; Carroll, L.; Andreani, L.C.; O'Brien, P. Co-optimizing grating couplers for hybrid integration of InP and SOI photonic platforms. *AIP Adv.* **2018**, *8*, 095109. <https://doi.org/10.1063/1.5046164>.

Disclaimer/Publisher's Note: The statements, opinions and data contained in all publications are solely those of the individual author(s) and contributor(s) and not of MDPI and/or the editor(s). MDPI and/or the editor(s) disclaim responsibility for any injury to people or property resulting from any ideas, methods, instructions or products referred to in the content.